



Published in final edited form as:

Mov Disord. 2021 March ; 36(3): 662–671. doi:10.1002/mds.28376.

Resting state functional connectivity predicts STN DBS clinical response

John R. Younce, M.D.¹, Meghan C. Campbell, Ph.D.^{1,3}, Tamara Hershey, Ph.D.^{2,3}, Aaron B. Tanenbaum, B.S.¹, Mikhail Milchenko, Ph. D.³, Mwiza Ushe, M.D.¹, Morvarid Karimi, M.D.^{*1}, Samer D. Tabbal, M.D.⁷, Albert E. Kim, M.D.¹, Abraham Z. Snyder, M.D. Ph.D.^{1,3}, Joel S. Perlmutter, M.D.^{1,2,3,4,5,6}, Scott A. Norris, M.D.^{1,3}

¹Washington University in St. Louis, Department of Neurology, St Louis, MO, USA

²Washington University in St. Louis, Department of Psychiatry, St Louis, MO, USA

³Washington University in St. Louis, Department of Radiology, St Louis, MO, USA

⁴Washington University in St. Louis, Department of Neuroscience, St Louis, MO, USA

⁵Washington University in St. Louis, Program in Physical Therapy, St Louis, MO, USA

⁶Washington University in St. Louis, Program in Occupational Therapy, St Louis, MO, USA

⁷American University of Beirut, Department of Neurology, Beirut, Lebanon

Abstract

Background: Deep brain stimulation of the subthalamic nucleus is a widely-used adjunctive therapy for motor symptoms of Parkinson disease, but with variable motor response. Predicting motor response remains difficult and novel approaches may improve surgical outcomes as well as understanding regarding pathophysiological mechanisms.

Objective: To determine whether pre-operative resting state functional connectivity MRI predicts motor response from deep brain stimulation of the subthalamic nucleus.

Methods: We collected preoperative resting-state functional MRI from 70 participants undergoing subthalamic nucleus deep brain stimulation. For this cohort, we analyzed strength of STN functional connectivity with seeds determined by stimulation-induced (ON/OFF) ¹⁵O H₂O PET regional cerebral blood flow differences in a partially overlapping group (n = 42). We correlated STN-seed functional connectivity strength with postoperative motor outcomes and applied linear regression to predict motor outcomes.

Results: Preoperative functional connectivity between left subthalamic nucleus and ipsilateral internal globus pallidus correlated with postsurgical motor outcomes ($r = -0.39$, $p = 0.0007$), with stronger preoperative functional connectivity relating to greater improvement. Left pallidal-

Correspondence to: Scott A Norris, M.D., Associate Professor, Washington University in St Louis, Department of Neurology, Box 8111, 660 S. Euclid Avenue, St. Louis, MO 63110, USA, Clinic: 314-362-6908, norriss@wustl.edu.
*deceased.

Author Contributions

JRY, MCC, TH, JSP, and SAN contributed to conception and design of the study; JRY, MCC, TH, ABT, MM, MU, SDT, AK, AZS, JSP, and SAN contributed to acquisition and analysis of data; JRY and SAN drafted the text and prepared the figures. All authors reviewed the manuscript and revised for intellectual content.

subthalamic nucleus connectivity also predicted motor response to DBS after controlling for covariates.

Interpretation: Preoperative pallidal-subthalamic nucleus resting-state functional connectivity predicts motor benefit from deep brain stimulation, though this should be validated prospectively before clinical application. These observations suggest that integrity of pallidal-subthalamic nucleus circuits may be critical to motor benefits from deep brain stimulation.

Keywords

DBS; Parkinson disease; functional connectivity

Introduction

Deep brain stimulation (DBS) of the subthalamic nucleus (STN) is a widely-used adjunct therapy for motor impairment in Parkinson disease (PD) but with substantial variability in degree of benefit^{1,2}. While levodopa responsiveness predicts some variability in STN DBS outcomes, an incomplete understanding of DBS predictors limits optimal delivery of this therapy^{3–6}. PET-based measures of relative regional cerebral blood flow (rCBF) responses to STN stimulation demonstrate local and downstream effects, including midbrain, thalamus, cerebellum, and prefrontal, motor, and temporal cortical regions^{7,8}. These STN stimulation-induced rCBF responses correlate with motor outcomes. Specifically, premotor and cerebellar responses correlate with gait, supplementary motor area with rigidity, and thalamus with bradykinesia^{8,9}. Correlations between rCBF and behavioral responses to STN stimulation imply network-level effects of STN DBS. This interpretation is supported by PET studies demonstrating modulation of PD-related metabolic brain networks from both DBS and neuromodulatory gene therapy at the STN, correlating with the effects of STN DBS on motor function and disability^{10,11}. Thus, modulation of PD-related networks may be important for DBS effects. Pre-operative evaluation of such networks may improve characterization of stimulation response and prediction of motor outcomes.

Resting-state functional connectivity MRI (rs-fcMRI) reflects the temporal correlations of spontaneous activity in blood oxygen level dependent (BOLD) signals across the brain, permitting organization into resting-state networks subserving various functions¹². Significant alterations in functional connectivity (FC) networks have been linked to PD manifestations^{13–15}. Various stimulation targets that are effective for treating parkinsonism are also highly functionally connected, implying that DBS may modulate networks to achieve its effects¹⁶. Furthermore, FC of stimulation location correlates with STN DBS effects in normative connectome data, supporting the notion that FC may correlate with STN DBS effects^{17,18}.

The most direct approach to determine the effects of DBS on resting state networks would be to perform rs-fcMRI studies after lead implantation. However, technical issues limit this approach. DBS electrodes produce a susceptibility artifact which obscures BOLD signals confounding FC measurements near electrodes and contact sites¹⁹. Furthermore, potential electrode heating raises safety concerns with current DBS electrodes within high field strength sequences used for BOLD imaging. While 3T MRI is standard for high quality rs-

fcMRI, structural and functional scans at 3T have been shown to exceed parameters recommended for DBS, which limits scan time and field strength for rs-fcMRI in DBS^{18,20,21}. Thus, alternative approaches evaluating FC in patients with DBS may improve analysis of DBS effects. Using brain regions known to respond to stimulation as seed regions to interrogate preoperative resting state rs-fcMRI may reveal functional network connectivity that predicts clinical response to DBS and avoids the technical limitations of post-operative MRIs.

We aimed to identify the relationship between preoperative rs-fcMRI and DBS motor response. To do this, we identified rCBF responses to STN stimulation using previously acquired ¹⁵O PET data. We then applied these response regions as seeds in a preoperative rs-fcMRI analysis. We hypothesized that connectivity patterns between regions modulated by STN stimulation would predict postoperative motor outcome from STN DBS.

Methods

Overview

From a prior ¹⁵O PET study with a stimulation on/off design, we identified brain regions with STN stimulation induced blood flow response. We then applied these regions as seeds in a partially overlapping cohort with preoperative (STN DBS) rs-fcMRI data (Figure 1). We correlated pre-operative functional connectivity between STN and seed regions with postoperative motor outcomes, defined as change in Unified Parkinson Disease Rating Scale part III (UPDRS-III). Significant correlations were then applied to a linear regression model to predict the postoperative change in UPDRS-III.

Participants

Participants were selected from a consecutive series of PD patients who had undergone bilateral STN DBS implantation surgery at the Movement Disorders Center in Washington University School of Medicine and who agreed to participate in this study. For each participant, the study included one or both of a) pre-operative rs-fcMRI, and b) post-operative PET (described below) and clinical measures of STN DBS effects. This research was approved by the Washington University Institutional Review Board, and written informed consent was obtained from each participant. Inclusion criteria for this study included diagnosis of idiopathic PD by UK Brain Bank criteria and placement of bilateral STN DBS between 2007 and 2017²². Exclusionary criteria included dementia, poor response to levodopa (except levodopa-resistant tremor), structural brain abnormalities, history of encephalitis, stroke, serious head injury or inability to hold the head still. Participants with metal or MRI-incompatible devices were excluded from rs-fcMRI.

Neurosurgical procedure

Patients with PD were pre-screened for comorbidities which would preclude safe electrode implantation and completed detailed formal neuropsychological testing to exclude dementia. All participants had bilateral STN DBS stimulators (Medtronic 3389 DBS leads paired the with most up-to-date internal pulse generators at the time of implantation: Activa™ SC, Kinetra™ SC, or Soletra™ SC) placed at Washington University as previously described²³.

Accurate electrode placement was verified by intraoperative microelectrode recordings, motor responses to intra-operative stimulation, and postoperative CT. DBS contacts were localized in atlas space using a previously validated method and compared with a probabilistic atlas of STN to confirm accurate placement^{24,25}. Participants with clear outlier electrodes (over 2 mm from STN target) or whose placement could not be confirmed by CT were removed from analysis.

PET methods

Post-operative PET data acquisition was performed as previously described, overlapping with previously reported research⁸. Briefly, following DBS implantation and clinical programming optimization, ¹⁵O PET scans were performed for each participant in the OFF-medication state (median 382.5 days after DBS, range 136–2513 days). PET scans were obtained in off-stimulation and unilateral ON-stimulation conditions, with side stimulated representing the more-affected brain hemisphere (determined by baseline UPDRS-III). Stimulation conditions included contacts targeting dorsal STN (D-STN) and contacts targeting ventral STN (V-STN), referred to collectively as ON-stimulation. Details regarding data acquisition, processing and quality assurance are found in Supplement S1.

MRI methods

MRI data were acquired preoperatively (median 12 days before DBS, range 1 to 295 days) using a Siemens 3T MAGNETOM Trio scanner. Scans were obtained ON-medication to minimize movement. Participants were asked to lie still in the scanner awake with their eyes closed. BOLD runs with visible body motion or where the participant reported sleep were discarded. Scans included a T1-weighted MPRAGE, a T2-weighted fast spin echo, and 1–3 rs-fcMRI BOLD EPI scans (7.3 min per run). Resting state fcMRI preprocessing and motion censoring were rigorously performed similar to previously described methods²⁶. Details regarding MRI acquisition and processing are found in Supplement S1.

Clinical evaluation

Preoperative and postoperative OFF-medication, ON-stimulation (postoperative) scores were collected from the 12 months before and after DBS implantation, and used to calculate average change in UPDRS-III over the study period. Average scores over the entire postoperative period were used to mitigate random fluctuations, to comprehensively represent overall postoperative performance, and to avoid bias in selecting which scores represented an “optimized” condition. Final UPDRS-III score at the end of the 12 month study period, and variability in UPDRS-III over the study period (calculated as within-subject standard deviation in UPDRS-III) were also computed. Levodopa equivalent daily doses (LEDD) at time of DBS surgery and 12 months postoperatively were also calculated, accounting for percent change across the timepoints²⁷. Scores for UPDRS part IV pertaining to dyskinesia were also totaled at the same time points. Full details are found in Supplement S1.

Statistical analysis

PET.—PET data were analyzed with SPM12 (<https://www.fil.ion.ucl.ac.uk/spm/>). Scans were flipped such that the stimulated side was placed on the left in all participants, and thus laterality concerned “ipsilateral and contralateral” rather than “left and right.” OFF-stimulation was compared with D-STN and V-STN stimulation conditions using paired-sample t-tests. Since D-STN and V-STN did not differ significantly, they were combined into ON-stimulation. Responses to DBS were determined in two ways: a priori-defined ROI analysis to maximize sensitivity at specific regions believed to respond to STN DBS, and whole-brain cluster analysis to capture responses outside of a priori-defined regions. A set of 33 ROIs were defined a priori based on a previous study demonstrating rCBF responses to STN DBS, as well as selected from regions hypothesized to be involved in the motor effects of PD, with overlapping ROIs removed (Supplement S2)^{7,28}. A 3 mm radius sphere was drawn for each ROI. We applied small-volume FWE correction to significant local maxima and corrected for total number of ROIs using the Benjamini-Hochberg false discovery rate (FDR). Whole-brain cluster-based analysis was used to identify significant responses after correction for family-wise error rate (FWE) of 0.05, and significant local maxima were identified within these clusters, with each local maxima identified as an area of DBS response. Local maxima within regions of significant response to STN stimulation identified from either the a priori ROI-based or cluster-based analysis were located in Talairach atlas space (using ICBM-152 transform). Ventrolateral (VL) thalamus was significant in both analyses and thus counted as a single area of response; the seed for lateral posterior thalamus largely overlapped that of VL thalamus, and was thus censored from further analyses. Thus, 12 anatomically unique regions of significant response remained and are hence-forth referred to as “DBS response seeds”^{29,30}. The seeds used for the cluster-based rCBF responses were the activation maps thresholded for significance at FWE-adjusted $p = 0.05$, and labelled by their predominant anatomic location.

Rs-fcMRI.—MRI data were analyzed using custom scripts in MATLAB 2014b (MathWorks, Inc) and FSL version 6.0³¹. For the rs-fcMRI analysis, we applied DBS response seeds from the PET analysis in addition to a probabilistic groupwise representation of STN stimulation sites. The latter was generated from individual participant contact #2 (targeting dorsolateral/motor STN in our implantation method) locations overlaid in atlas space and thresholded per voxel to include a minimum of 5 participants per voxel. Because rCBF-defined seeds were obtained from unilateral stimulation while clinical DBS effects are the result of bilateral stimulation, we mirrored these seeds across midline for rs-fcMRI correlation with clinical motor effects. Then, the functional connectivity between each STN and the set of 12 DBS response seeds was computed. Correlation maps were generated by extracting the BOLD time course from each seed, and the Pearson correlation coefficient (r) was computed between the time course of each seed pair. Correlation coefficients were then Fisher z-transformed and a correlation matrix between each seed pair was obtained. Connectivity between each STN and each DBS response seed was then correlated to overall change in UPDRS-III (primary outcome), as well final change and variability in UPDRS-III (secondary outcomes). We analyzed motor ratings within SPSS 25 (IBM Corp, 2017). Paired-sample t-tests were used to compare motor data between pre-DBS and post-DBS conditions. Pearson correlations between motor ratings, levodopa dose and response, and FC

were performed to analyze the contributing effect of preoperative clinical variables on the above analyses. Pearson correlations between FC and post-operative change in LEDD and FC and post-operative change in UPDRS IV dyskinesia scores were also calculated as secondary outcomes. Multiple comparisons were FDR-corrected at 0.05 for the number of correlations within each analysis.

For correlations between FC and change in UPDRS-III that were significant after multiple comparison correction, a linear regression model was used to predict change in UPDRS-III using these significant FC relationships. Covariates included age, sex, handedness, maximally affected side, levodopa equivalent daily dose (LEDD) at time of DBS implantation, and baseline UPDRS-III. Assumptions checked included linearity of data, homoscedasticity, normality of residuals, and absence of outliers, autocorrelation and multicollinearity. Hierarchical linear regression was used to compare the model including clinical predictors with the model including only the FC predictor. Cross-validation within the dataset was performed using a leave-one-out approach, with mean absolute error and root mean square error used to evaluate model validity. To test the predictive power of FC in addition to preoperative ON/OFF levodopa response, linear models (using the above covariates) predicting change in UPDRS-III using preoperative ON/OFF levodopa response with and without significant FC relationships were compared using hierarchical linear regression.

An exploratory rs-fcMRI analysis was also performed to investigate relationships between UPDRS-III and FC at a whole-brain level. Global resting state correlation maps were calculated for four seeds: left STN, right STN, left GPI and right GPI to explore asymmetry in correlations between motor outcomes and STN-GPI connectivity. These were used to create a general linear model (GLM) with change in UPDRS-III as the explanatory variable. FSL randomise was used to compute T-maps for this GLM thresholded to a T-statistic of 2.0, and cluster-wise significance testing at $p = 0.05$ was performed using 5000 permutations.

Results

Participants: Forty-two of 73 participants that had postoperative PET scans passed quality criteria in OFF-stimulation and at least one ON-stimulation condition (see “PET methods”). Seventy-six of 103 participants that completed preoperative rs-fcMRI passed quality criteria (see “MRI methods”) and 70 were included in outcomes analysis. Of those removed from analysis, 1 had insufficient preoperative records, 1 died shortly after DBS due to surgical complications, and 4 had inaccurate electrode implantations (Supplement S3). Clinical characteristics and scores before and after DBS for participants included in the imaging cohorts are summarized in Table 1. Baseline characteristics were similar between PET and rs-fcMRI groups. Mean lesion effect on UPDRS III prior to stimulation was small (-2.2 points). Mean UPDRS-III, LEDD, and UPDRS-IV dyskinesia scores all decreased over the first year post-DBS with clinically programmed stimulation settings (Table 1). Preoperative ON/OFF levodopa change in UPDRS-III correlated with post-operative change in UPDRS-III ($r = 0.41$, $p < 0.001$).

PET rCBF responses to STN stimulation: Unilateral STN stimulation produced significant responses in 12 regions in both ROI-based and whole-brain analyses, including cortical, thalamic and basal ganglia regions. Significant clusters observed in the whole-brain analysis are shown in Figure 2, where STN stimulation decreased rCBF in sensorimotor cortical regions, and increased rCBF in thalamic regions. A full list of ROIs and rCBF stimulation response locations may be found in Supplement S2 and S4.

rs-fcMRI Analysis: The FC matrix between STN and DBS response seeds is shown in Figure 3a, and the same matrix with each FC relationship correlated to change in UPDRS-III is shown in Figure 3b. FC of left STN to left GPI significantly correlated with overall change in UPDRS-III ($r = -0.39$, $p = 0.001$, Figure 2c). Connectivity between left STN and left thalamus also correlated with change in UPDRS-III ($r = -0.33$, $p = 0.006$), although this was not significant after multiple comparison correction. Of note, right STN to right GPI connectivity was not significantly correlated with change in UPDRS-III. A full list of correlations between FC and change in UPDRS-III is found in Table 2.

Left STN-GPi FC also correlated with final change in UPDRS-III ($r = -0.38$, $p = 0.001$), but did not correlate with variability in UPDRS-III ($r = -0.042$). Left STN-GPi FC did not correlate with baseline UPDRS-III ($r = -0.012$), preoperative daily levodopa equivalent dose (LEDD) ($r = -0.017$), or levodopa response ($r = -0.089$). FC did not significantly correlate with post-DBS LEDD reduction or change in UPDRS-IV dyskinesia scores. Minimal effects on the correlation between left STN-GPi FC and overall change in UPDRS-III were observed when participants censored due to poor electrode placement were included ($r = -0.393$).

A linear regression analysis with covariates of age, sex, handedness, maximum affected side, baseline UPDRS-III, and LEDD demonstrated that left STN-GPi FC predicted change in UPDRS-III (overall model: $R^2 = 0.26$, $F = 3.1$, $p = 0.007$; L STN-GPi FC as predictor: $\beta = -0.40$, $p < 0.001$). The model including these clinical variables did not predict significantly more variance in motor outcomes than L STN-GPi FC alone (F -change = 1.5, $p = 0.179$). Cross-validated error was modest for this model, with mean absolute error of 11.7 ± 9.5 (percent change UPDRS-III) and root mean square error of 15.0. A model including both preoperative ON/OFF levodopa response and left STN-GPi FC with the above covariates predicted significantly more variance in outcome than the model without FC (F -change 12.5, $p < 0.001$).

Exploratory analysis relating change in UPDRS-III with whole-brain connectivity to STN and GPi did not reveal significant clusters (Supplement S5). Left STN connectivity to a region primarily involving ipsilateral pallidum and putamen showed non-significant correlation with a reduction in UPDRS-III, while this did not hold true for right STN. GPi connectivity to ipsilateral STN and surrounding midbrain regions demonstrated similar asymmetry.

Discussion

We investigated preoperative rs-fcMRI relationships to STN DBS motor outcomes using rCBF data to select regions responding to STN stimulation as seeds. We found that preoperative left pallidal-subthalamic FC predicts motor outcomes of STN DBS.

Study Limitations and Strengths

This study integrates PET, rs-fcMRI, and DBS to predict DBS motor outcomes using preoperative FC. Although the preoperative nature of this rs-fcMRI dataset makes it useful for prediction, this also limits its utility in exploring DBS mechanisms. A key caveat of this study is the role of laterality in both PET and rs-fcMRI data. As participants were stimulated unilaterally on their more affected side during PET acquisition, images had to be flipped along the x-axis to standardize stimulation to permit averaging across all participants, thus identifying rCBF responses as “ipsilateral” or “contralateral,” rather than “left” or “right.” This may obscure responses in brain regions without symmetric connectivity to STN, and thus the clear asymmetry seen in the rs-fcMRI data could not be verified in our PET data. The effects of bilateral stimulation may not be fully represented by unilateral stimulation parameters, thus limiting the set of brain regions applied to rs-fcMRI data and clinical outcomes. While our approach was conservative, under more robust clinical stimulation parameters a larger set of responses could provide additional regions and networks to explore. Furthermore, while PET data were acquired OFF-medication to maximize the effect of STN DBS, rs-fcMRI data were acquired ON-medication due to technical limitations of scanning PD patients in the OFF state. While levodopa likely has little effect on FC in early PD, its effects on FC in advanced PD remain uncertain and may limit the interpretation regarding lack of correlation between STN-GPi FC and baseline UPDRS-III³². Another caveat is that we had too limited an overlap of participants having BOLD MRI and those having PET to directly analyze rs-fcMRI connectivity and blood flow responses using a within-subjects analysis. Additionally, although all participants were programmed by the same group of clinicians using a consistent approach, individual variation in programming effectiveness could not be specifically accounted for. Finally, although cross-validation within the dataset produced modest error, replication in a test cohort will be necessary prior to use as a biomarker.

The key strength of this study is its multimodal nature, integrating PET, rs-fcMRI, and DBS in a novel fashion to demonstrate that individual variability in resting-state FC of the STN is predictive of motor benefit in STN DBS. This study is strengthened by its technical quality, including BOLD rs-fcMRI processing with rigorous motion censoring. Censoring data contaminated by motion is of paramount importance in studying movement disorders using rs-fcMRI, as movement may cause spurious correlations and artifacts in a systematic manner corresponding to disease severity and state changes. Studying participants with advanced PD requiring DBS may increase FC differences compared to earlier stages of PD³³.

Preoperative functional connectivity predicts DBS motor effects

STN and GPi are highly connected anatomically and functionally, with GPi acting as the principal output nucleus of the basal ganglia and STN among its chief modulators with

direct connection via the subthalamic fasciculus^{34,35}. STN and GPI are the two DBS targets with established efficacy for motor symptoms of PD, and may share certain pathophysiological characteristics in PD^{36–38}. The revelation that the preoperative STN-GPI FC predicts DBS-related improvement in motor parkinsonism further suggests that preoperative pallidal-subthalamic functional interactions relate to the motor effect of STN DBS. Although the cause of variability in pallidal-subthalamic FC is unclear, contributions from neurodegenerative and genetic factors are quite plausible. While FC of postoperative stimulation locations has previously been related to DBS motor outcomes using normative connectome data (thus negating any individual differences in preoperative FC), this study differs from previous attempts in that it demonstrates that individual differences in preoperative connectivity patterns between DBS candidates are also predictive of outcome¹⁷. STN-GPI FC may thus offer promise as a biomarker for STN DBS responsiveness, used in conjunction with more established predictors such as levodopa responsiveness. Integration of this marker with other predictors of DBS responsiveness may be particularly powerful as a predictive tool in the clinical setting, as illustrated by the increased predictive power of the model using FC in addition to levodopa response as compared to medication response alone³⁹. However, this requires future prospective validation at the individual level, a promising approach undergoing development⁴⁰.

Asymmetry of connectivity and DBS response

While left STN connectivity with left GPi robustly correlated with motor outcomes, it is unclear why the same did not hold true for right STN to right GPi connectivity. Even when controlled for handedness and most affected side, only left pallidal-subthalamic connectivity predicted outcomes. We expected STN connectivity to relate to motor outcomes symmetrically, however the role of laterality and stimulation side in the effect of STN DBS is complex. Although early studies in STN DBS showed only contralateral reduction in rigidity and bradykinesia, subsequent data support a substantial ipsilateral effect on parkinsonism⁹. Furthermore, even unilateral STN DBS may be sufficient to treat parkinsonian symptoms in some patients⁴¹. This may be a manifestation of an asymmetric relationship between STN and motor activity in PD⁴². In some patients a “dominant STN” has been observed, where unilateral STN stimulation produces a similar effect to bilateral stimulation⁴³. In one experiment in PD patients receiving STN DBS, phase coupling of bilateral STN occurred with movement of either hand, but flow of synchronization was always from right to left STN regardless of which hand was moved⁴⁴. The distinction between the left and right STN connectivity relationship with motor outcomes here suggests that these observations may represent asymmetric motor circuits modulated by STN stimulation. Further study is needed to explore the relationship between connectivity and symmetry in STN DBS.

In conclusion, brain regions with altered blood flow response secondary to STN stimulation, specifically GPi, demonstrate altered preoperative resting-state FC that relates to motor outcomes following STN DBS. Our results suggest that integrity of STN-GPI FC is important in predicting motor outcomes from STN DBS. With continued study, FC may become a valuable tool for presurgical planning, including identification of DBS candidates and response prediction.

Supplementary Material

Refer to Web version on PubMed Central for supplementary material.

Acknowledgments

We would like to thank the following people for their help with this project: JoAnn Antenor, Hugh Flores (image processing), Tom Videen (development of processing pipelines), Johanna Hartlein, Dawn Keilbach, Jill Smith, and Angela Wernle (recruitment and data collection), Hussain Jafri (data collection), Matthew Brier, Aimee Morris, and John O'Donnell (discussion).

Financial disclosure/Conflict of Interest: The authors do not have any financial disclosures or conflicts of interest other than the funding sources listed below.

Funding sources for study: National Institutes of Health; R01 NS41509; NS41248; NS58797; NS075321, NS103957, NS107281, NS092865, NS097437, NS097799, NS075527; NS109487, 1U10NS077384, U54NS116025, U19NS110456; F31 NS071639; CO6 RR020092; R01 AG050263; T32 EB021955, P30NS98577, CTSA at Washington University (UL1TR000448); Brain & Behavior Research Foundation (NARSAD) Young Investigator Award; American Parkinson Disease Association (APDA) Advanced Research Center for PD at WUSTL; Greater St. Louis Chapter of the APDA; Barnes Jewish Hospital Foundation (Clinical Translational Research Award; Elliot Stein Family Fund; PD Research Fund); Paula C and Rodger O Riney Fund, the Jo Oertli fund, and the Scott G. Lentini fund.

Financial Disclosures of All Authors (for the preceding 12 months)

JRY – Washington University School of Medicine (employment); NIH T32 EB021955 (research support); International Parkinson and Movement Disorder Society (travel grant)

MCC – Washington University School of Medicine (employment); McDonnell Center for Systems Neuroscience at Wash U, Mallinckrodt Institute of Radiology at Wash U pilot project grant, Neuroimaging Laboratory at Wash U Innovation pilot grant, Biomarkers Across Neurodegenerative Diseases program funded by the Alzheimer's Association and MJ Fox Foundation, NIH R01 NS097437, R01 NS075321, R01 NS097799, R21 AG063974, R61 AT010753 (research support); Parkinson Foundation (honoraria)

TH – Washington University School of Medicine (employment); NIH R01 HD070855, R01 DK064832, R01 HD085930, R01 ES025991, R01 ES029524, P01 NS080675, R01 OH11661, UH2 TR002065, P30 NS098577, R01 NS109487 (research support); University of Catania, Earlham College, Wolfram Syndrome Annual Conference (honoraria)

ABT – Washington University School of Medicine (employment)

MM – Washington University School of Medicine (employment); NIH U24 CA204854, P30 NS048056, R01 EB009352, R01 NS109487 (research support)

MU – Washington University School of Medicine (employment); NIH (R01 NS109487)

MK – none

SDT – American University of Beirut (employment); International Parkinson and Movement Disorder Society (honorarium)

AEK – Dana Farber Cancer Institute and Massachusetts General Hospital (employment); American Brain Tumor Association Basic Research Fellowship in honor of Paul Fabbri (research support)

AZS – Washington University School of Medicine (employment), NIH (P30 NS98577)

JSP – Washington University School of Medicine (employment); Michael J Fox Foundation, Barnes-Jewish Hospital Foundation - Elliot Stein Family Fund and Parkinson disease research fund, American Parkinson Disease Association Advanced Research Center at Washington University, Greater St. Louis Chapter of the APDA, Paula and Rodger Riney Fund, Jo Oertli Fund, Huntington Disease Society of America, Murphy Fund, CHDI, Department of Defense DOD W81XWH-217-1-0393, NIH NS075321, NS103957, NS107281, NS092865, U10NS077384, NS097437, U54NS116025, U19 NS110456, AG050263, AG-64937, NS097799, NS075527, ES029524, NS109487, R61 AT010753 (research support); Dystonia Coalition – supported by NIH NS116025, NS065701, TR001456 (co-director); Dystonia Medical Research Foundation (Director of Medical and Scientific Advisory Committee);

Parkinson Study Group (Chair of the Scientific Advisory Committee); Huntington Study Group (Chair of the Standards Committee and member of the Education Committee); American Parkinson Disease Association (Scientific Advisory Board); ENROLL-HD (Chair of the Scientific and Publication Committee); CHDI, Huntington Disease Study Group, Parkinson Study Group, Beth Israel Hospital, U Pennsylvania, Stanford U (honoraria); Wood, Cooper and Peterson, LLC, and Simmons and Simmons LLP (medical-legal consultation).

SAN – Washington University School of Medicine (employment); Dystonia Medical Research Foundation, Scott G. Lentin fund, NIH R01 NS103957, TR00145609 (research support)

References

1. Deuschl G, Schade-Brittinger C, Krack P, et al. A randomized trial of deep-brain stimulation for Parkinson's disease. *N. Engl. J. Med.* 2006;355(9):896–908. [PubMed: 16943402]
2. Follett KA, Weaver FM, Stern M, et al. Pallidal versus subthalamic deep-brain stimulation for Parkinson's disease. *N. Engl. J. Med.* 2010;362(22):2077–2091. [PubMed: 20519680]
3. Stefani A, Cerroni R, Mazzone P, et al. Mechanisms of action underlying the efficacy of deep brain stimulation of the subthalamic nucleus in Parkinson's disease: central role of disease severity. *Eur. J. Neurosci.* 2019;49(6):805–816. [PubMed: 30044030]
4. Lozano AM, Lipsman N. Probing and regulating dysfunctional circuits using deep brain stimulation. *Neuron* 2013;77(3):406–24. [PubMed: 23395370]
5. Welter ML, Houeto JL, Tezenas du Montcel S, et al. Clinical predictive factors of subthalamic stimulation in Parkinson's disease. *Brain* 2002;125(Pt 3):575–83. [PubMed: 11872614]
6. Tsai S-T, Lin S-H, Chou Y-C, et al. Prognostic factors of subthalamic stimulation in Parkinson's disease: a comparative study between short- and long-term effects. *Stereotact. Funct. Neurosurg.* 2009;87(4):241–8. [PubMed: 19556833]
7. Hershey T, Revilla FJ, Wernle AR, et al. Cortical and subcortical blood flow effects of subthalamic nucleus stimulation in PD. *Neurology* 2003;61(6):816–21. [PubMed: 14504327]
8. Hill KK, Campbell MC, McNeely ME, et al. Cerebral blood flow responses to dorsal and ventral STN DBS correlate with gait and balance responses in Parkinson's disease. *Exp. Neurol.* 2013;241(1):105–12. [PubMed: 23262122]
9. Tabbal SD, Ushe M, Mink JW, et al. Unilateral subthalamic nucleus stimulation has a measurable ipsilateral effect on rigidity and bradykinesia in Parkinson disease. *Exp. Neurol.* 2008;211(1):234–42. [PubMed: 18329019]
10. Asanuma K, Tang C, Ma Y, et al. Network modulation in the treatment of Parkinson's disease. *Brain* 2006;129(Pt 10):2667–78. [PubMed: 16844713]
11. Feigin A, Kaplitt MG, Tang C, et al. Modulation of metabolic brain networks after subthalamic gene therapy for Parkinson's disease. *Proc. Natl. Acad. Sci. U. S. A.* 2007;104(49):19559–64. [PubMed: 18042721]
12. Fox MD, Zhang D, Snyder AZ, Raichle ME. The global signal and observed anticorrelated resting state brain networks. *J. Neurophysiol.* 2009;101(6):3270–83. [PubMed: 19339462]
13. Gratton C, Koller JM, Shannon W, et al. Emergent Functional Network Effects in Parkinson Disease. *Cereb. Cortex* 2018;1–15. [PubMed: 29253248]
14. Baudrexel S, Witte T, Seifried C, et al. Resting state fMRI reveals increased subthalamic nucleus-motor cortex connectivity in Parkinson's disease. *Neuroimage* 2011;55(4):1728–38. [PubMed: 21255661]
15. Kurani AS, Seidler RD, Burciu RG, et al. Subthalamic nucleus--sensorimotor cortex functional connectivity in de novo and moderate Parkinson's disease. *Neurobiol. Aging* 2015;36(1):462–9. [PubMed: 25095723]
16. Fox MD, Buckner RL, Liu H, et al. Resting-state networks link invasive and noninvasive brain stimulation across diverse psychiatric and neurological diseases. *Proc. Natl. Acad. Sci.* 2014;111(41):E4367–E4375. [PubMed: 25267639]
17. Horn A, Reich M, Vorwerk J, et al. Connectivity Predicts deep brain stimulation outcome in Parkinson disease. *Ann. Neurol.* 2017;82(1):67–78. [PubMed: 28586141]
18. Horn A, Wenzel G, Irmen F, et al. Deep brain stimulation induced normalization of the human functional connectome in Parkinson's disease. *Brain* 2019;1–15. [PubMed: 30596908]

19. In M-H, Cho S, Shu Y, et al. Correction of metal-induced susceptibility artifacts for functional MRI during deep brain stimulation. *Neuroimage* 2017;158(10):26–36. [PubMed: 28666879]
20. Medtronic. MRI Guidelines for Medtronic deep brain stimulation systems. 2015;
21. Carmichael DW, Pinto S, Limousin-Dowsey P, et al. Functional MRI with active, fully implanted, deep brain stimulation systems: safety and experimental confounds. *Neuroimage* 2007;37(2):508–17. [PubMed: 17590355]
22. Hughes AJ, Daniel SE, Kilford L, Lees AJ. Accuracy of clinical diagnosis of idiopathic Parkinson's disease: a clinico-pathological study of 100 cases. *J. Neurol. Neurosurg. Psychiatry* 1992;55:181–184. [PubMed: 1564476]
23. Tabbal SD, Revilla FJ, Mink JW, et al. Safety and efficacy of subthalamic nucleus deep brain stimulation performed with limited intraoperative mapping for treatment of Parkinson's disease. *Neurosurgery* 2007;61(3 Suppl):119–27; discussion 127–9. [PubMed: 17876242]
24. Milchenko M, Snyder AZ, Campbell MC, et al. ESM-CT: a precise method for localization of DBS electrodes in CT images. *J. Neurosci. Methods* 2018;308:366–376. [PubMed: 30201271]
25. Milchenko M, Norris SA, Poston K, et al. 7T MRI subthalamic nucleus atlas for use with 3T MRI. *J. Med. imaging (Bellingham, Wash.)* 2018;5(1):015002.
26. Raut RV, Mitra A, Snyder AZ, Raichle ME. On time delay estimation and sampling error in resting-state fMRI. *Neuroimage* 2019;194(November 2018):211–227. [PubMed: 30902641]
27. Tomlinson CL, Stowe R, Patel S, et al. Systematic review of levodopa dose equivalency reporting in Parkinson's disease. *Mov. Disord.* 2010;25(15):2649–53. [PubMed: 21069833]
28. DeLong MR. Primate models of movement disorders of basal ganglia origin. *Trends Neurosci.* 1990;13(7):281–5. [PubMed: 1695404]
29. Lancaster JL, Woldorff MG, Parsons LM, et al. Automated Talairach atlas labels for functional brain mapping. *Hum. Brain Mapp.* 2000;10(3):120–31. [PubMed: 10912591]
30. Lancaster JL, Tordesillas-Gutiérrez D, Martínez M, et al. Bias between MNI and Talairach coordinates analyzed using the ICBM-152 brain template. *Hum. Brain Mapp.* 2007;28(11):1194–205. [PubMed: 17266101]
31. Jenkinson M, Beckmann CF, Behrens TEJ, et al. FSL. *Neuroimage* 2012;62(2):782–90. [PubMed: 21979382]
32. White RL, Campbell MC, Yang D, et al. Little Change in Functional Brain Networks Following Acute Levodopa in Drug-Naïve Parkinson's Disease. *Mov. Disord.* 2020;35(3):499–503. [PubMed: 31854465]
33. Olde Dubbelink KTE, Stoffers D, Deijen JB, et al. Resting-state functional connectivity as a marker of disease progression in Parkinson's disease: A longitudinal MEG study. *NeuroImage. Clin.* 2013;2(1):612–9. [PubMed: 24179812]
34. Pujol S, Cabeen R, Sébille SB, et al. In vivo Exploration of the Connectivity between the Subthalamic Nucleus and the Globus Pallidus in the Human Brain Using Multi-Fiber Tractography. *Front. Neuroanat.* 2016;10(January):119. [PubMed: 28154527]
35. Rodriguez-Sabate C, Morales I, Lorenzo JN, Rodriguez M. The organization of the basal ganglia functional connectivity network is non-linear in Parkinson's disease. *NeuroImage. Clin.* 2019;22:101708. [PubMed: 30763902]
36. Litvak V, Jha A, Eusebio A, et al. Resting oscillatory cortico-subthalamic connectivity in patients with Parkinson's disease. *Brain* 2011;134(Pt 2):359–74. [PubMed: 21147836]
37. Wang DD, de Hemptinne C, Miocinovic S, et al. Pallidal Deep-Brain Stimulation Disrupts Pallidal Beta Oscillations and Coherence with Primary Motor Cortex in Parkinson's Disease. *J. Neurosci.* 2018;38(19):4556–4568. [PubMed: 29661966]
38. Kühn AA, Kempf F, Brücke C, et al. High-frequency stimulation of the subthalamic nucleus suppresses oscillatory beta activity in patients with Parkinson's disease in parallel with improvement in motor performance. *J. Neurosci.* 2008;28(24):6165–73. [PubMed: 18550758]
39. Wong JK, Middlebrooks EH, Grewal SS, et al. A Comprehensive Review of Brain Connectomics and Imaging to Improve Deep Brain Stimulation Outcomes. *Mov. Disord.* 2020;35(5):741–751. [PubMed: 32281147]
40. Gordon EM, Laumann TO, Gilmore AW, et al. Precision Functional Mapping of Individual Human Brains. *Neuron* 2017;95(4):791–807.e7. [PubMed: 28757305]

41. Sung VW, Watts RL, Schrandt CJ, et al. The relationship between clinical phenotype and early staged bilateral deep brain stimulation in Parkinson disease. *J. Neurosurg.* 2013;119(6):1530–6. [PubMed: 24074493]
42. Lizarraga KJ, Luca CC, De Salles A, et al. Asymmetric neuromodulation of motor circuits in Parkinson’s disease: The role of subthalamic deep brain stimulation. *Surg. Neurol. Int.* 2017;8:261. [PubMed: 29184712]
43. Castrioto A, Meaney C, Hamani C, et al. The dominant-STN phenomenon in bilateral STN DBS for Parkinson’s disease. *Neurobiol. Dis.* 2011;41(1):131–7. [PubMed: 20826212]
44. Darvas F, Hebb AO. Task specific inter-hemispheric coupling in human subthalamic nuclei. *Front. Hum. Neurosci.* 2014;8(September):701. [PubMed: 25249965]

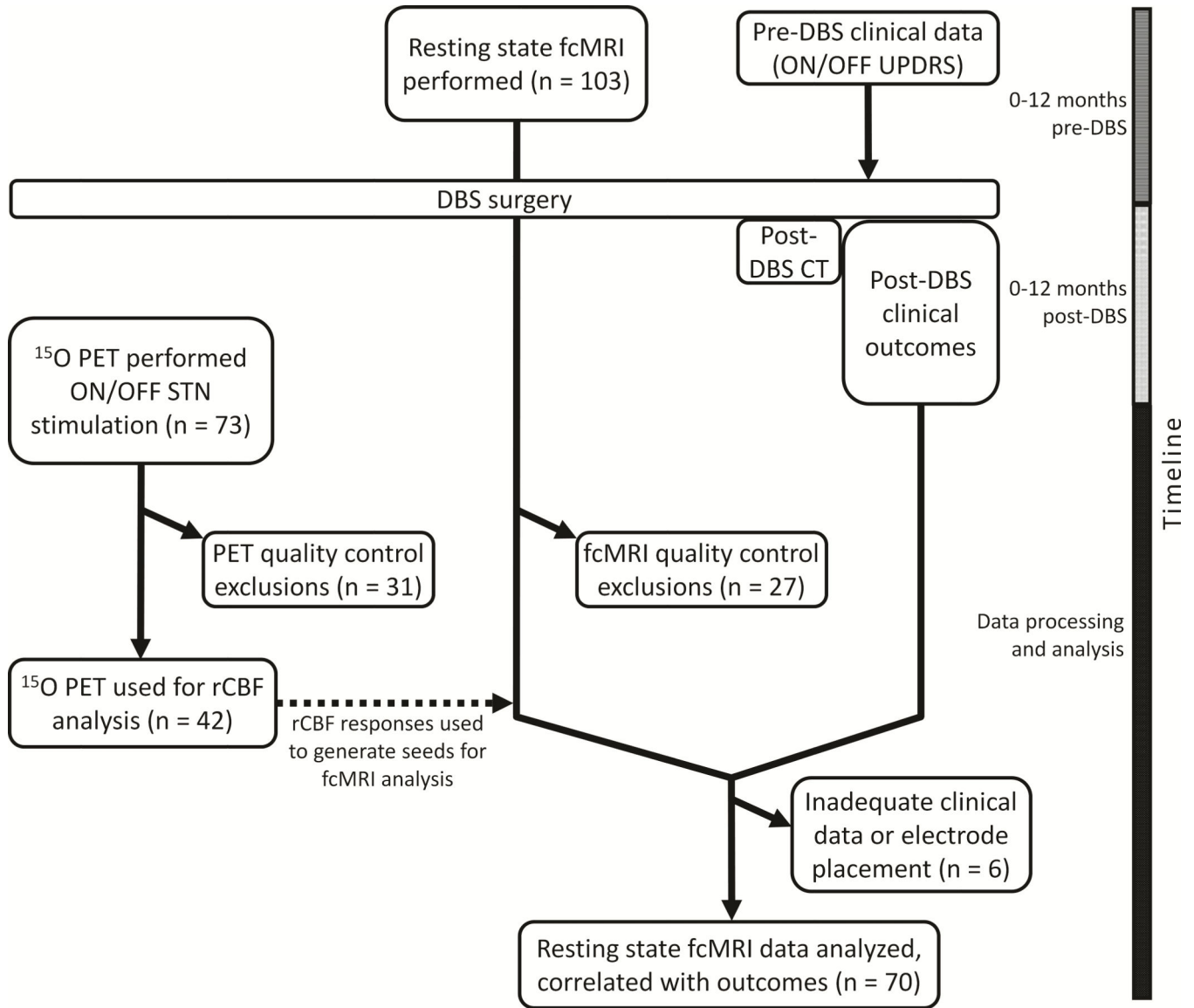


Figure 1: Study flowchart. Each imaging modality (rs-fcMRI and PET) occurred as independent components of a larger DBS outcome study focused on clinical outcomes (322 participants enrolled between 2007–2017). The PET component was performed only between 2009 and 2015. 19 participants received both rs-fcMRI and PET and passed all quality-control criteria for study inclusion.

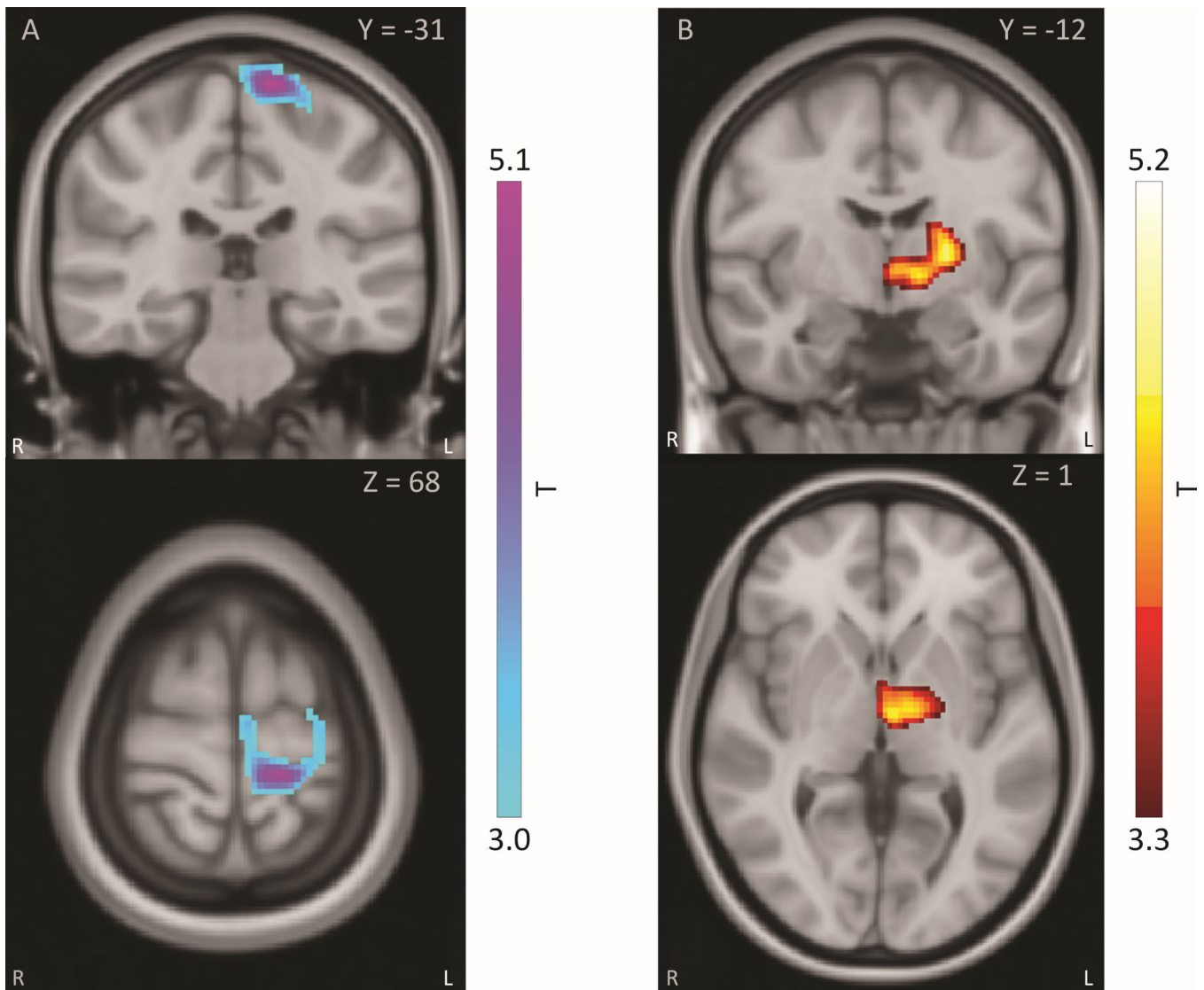


Figure 2:

PET rCBF responses to unilateral STN stimulation in whole-brain analysis. Responses shown are significant at cluster-wise FWE $p < 0.05$. Side ipsilateral to stimulation is displayed as standard radiological left (figure right). Reference atlas is in Talairach space.

A: STN stimulation produced negative rCBF response centered in ipsilateral dorsal sensorimotor regions, including primary motor, primary sensory, and SMA cortex. B: STN stimulation produced positive rCBF response centered in ipsilateral thalamus, including ventrolateral and mediodorsal regions. Scale is in t-statistic for paired T-test between stimulation condition and OFF condition. Voxels displayed are thresholded to cluster-wise FWE-corrected significance at $p < 0.05$.

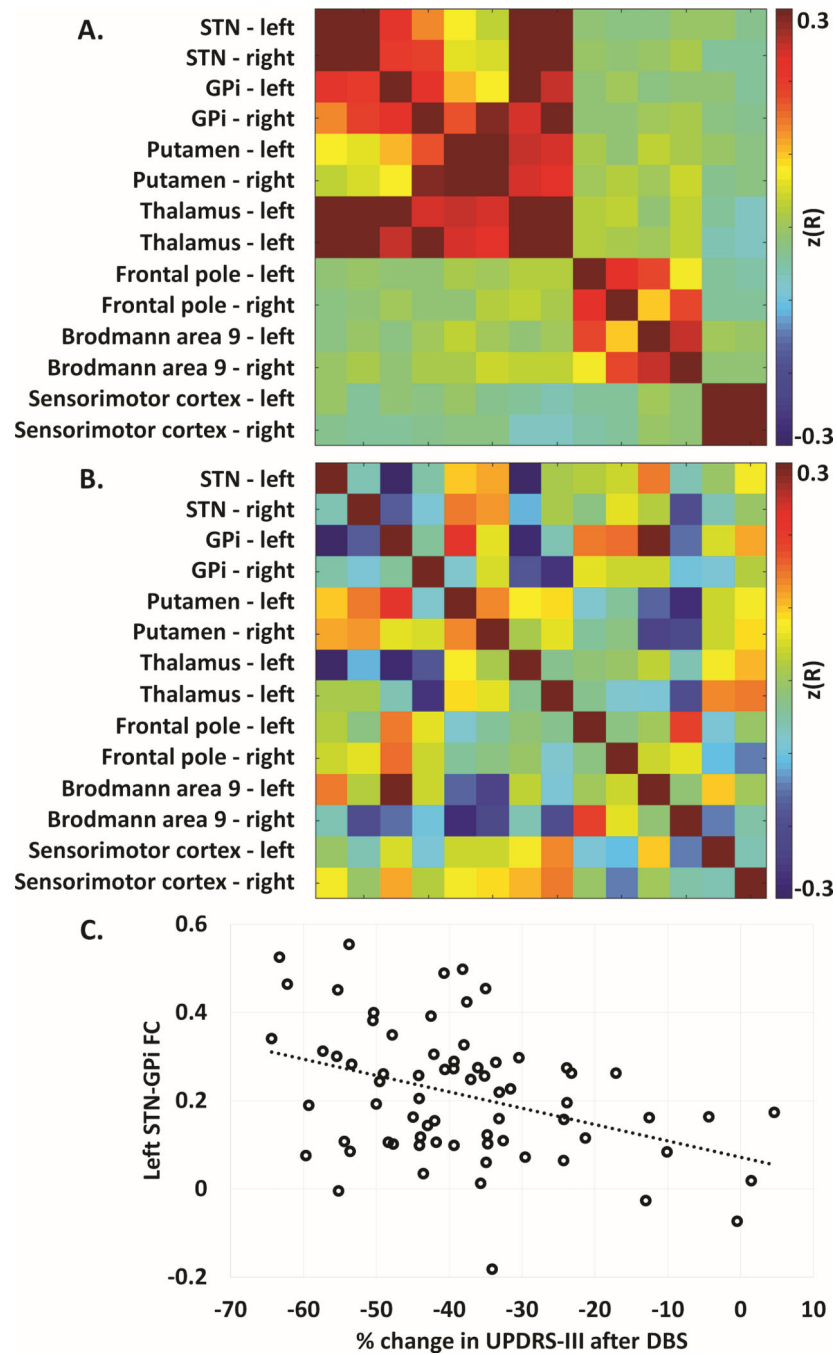


Figure 3: Resting state fMRI connectivity matrices. A: Z-transformed correlation matrix of all regions of PET defined DBS response, mirrored in contralateral hemisphere and inclusive of bilateral STN, for all DBS subjects. B: Matrix in (A) correlated with percent change UPDRS-III. C: Scatterplot of left STN – left GPI FC versus percent change UPDRS-III ($r = -0.385$, $p = 0.001$).

Table 1:

A. Clinical characteristics of participants receiving pre-DBS rs-fcMRI for primary outcome measurement and B. participants receiving ^{15}O PET with unilateral STN stimulation to determine rs-fcMRI seed placement. Relevant values are reported as mean \pm standard deviation. OFF-medication was defined as the practically-defined OFF state with overnight medication withdrawal. Postoperative UPDRS-III values are ON-stimulation with bilateral clinical stimulation settings and averaged over first year after DBS. The participants receiving ^{15}O PET were similar to the participants receiving fcMRI in age, baseline UPDRS-III, and motor response to DBS.

A.	
Participants receiving preoperative rs-fcMRI (n = 70)	
Sex	46 male, 24 female
Age at DBS (years)	62.8 \pm 9.3
UPDRS-III (preoperative) ON-medication	18.0 \pm 6.9
UPDRS-III (preoperative) OFF-medication	35.4 \pm 7.3
UPDRS-III response to levodopa (pre-DBS) (%)	-49.2 \pm 16
Change in UPDRS-III after DBS (%) OFF-medication	-38.1 \pm 15
LEDD at DBS (mg)	1708 \pm 662
LEDD at 12 months post-DBS (mg)	1106 \pm 480
Dyskinesia score pre-DBS	2.7 \pm 1.8
Dyskinesia score post-DBS	0.7 \pm 0.8
Mean DBS voltage (V)	2.69 \pm 0.6
Mean DBS frequency (Hz)	177 \pm 19
Mean DBS pulse width (μs)	60.6 \pm 4.4
B.	
Participants receiving postoperative ^{15}O PET (n = 42)	
Sex	25 male, 17 female
Age at DBS (years)	61.8 \pm 8.9
Age at PET (years)	63.3 \pm 8.9
UPDRS-III (preoperative) OFF-medication	36.1 \pm 10.2
Change in UPDRS-III after DBS (%) OFF-medication	-36.8 \pm 22*

Table 2:

Correlations between change in UPDRS-III after DBS with resting state FC of STN and brain regions modulated by DBS. All values displayed with Pearson correlation coefficient (r) and uncorrected p-value. Negative correlations indicate that greater motor benefit correlates with higher connectivity, as an improvement in UPDRS-III is a negative change.

	Left STN		Right STN	
	R	p	R	p
Internal globus pallidus – left	-0.394 **	0.0007	-0.176	0.144
Internal globus pallidus – right	-0.058	0.633	-0.093	0.445
Putamen – left	0.103	0.397	0.144	0.235
Putamen – right	0.113	0.35	0.125	0.303
Thalamus – left	-0.326 *	0.006	-0.119	0.329
Thalamus – right	0.01	0.932	0.009	0.944
Frontal pole – left	0.021	0.862	-0.02	0.867
Frontal pole – right	0.043	0.725	0.058	0.634
Brodman area 9 – left	0.145	0.233	0.023	0.853
Brodman area 9 – right	-0.065	0.595	-0.199	0.099
Sensorimotor cortex – left	-0.007	0.954	-0.057	0.637
Sensorimotor cortex – right	0.067	0.58	-0.006	0.958

* denotes significant correlations at $p < 0.05$ before correction for multiple comparisons.

** denotes significant correlations at $p < 0.05$ after FDR correction for multiple comparisons.